Bulletin of Electrical Engineering and Informatics
Vol. 10, No. 4, August 2021, pp. 1960~1967
ISSN: 2302-9285, DOI: 10.11591/eei.v10i4.3084

Triple-layer remote phosphor structure: a selection of the higher color quality and lumen efficiency for WLEDs

Phan Xuan Le, Le Hung Tien
Faculty of Engineering, Van Lang University, Viet Nam

Article Info

Article history:

Received Dec 14, 2020
Revised Apr 18, 2021
Accepted Jun 14, 2021

Keywords:

Color quality
Dual-layer phosphor
Luminous efficacy
Remote-phosphor
Triple-layer phosphor

ABSTRACT

To enhance color quality of glass-based phosphor-converted white light-emitting diodes (pc-WLEDs) with multi-layer remote phosphor layer structures, two phosphors, green CdS:In and red ZnS:Te,Mn, are integrated into the glass matrix and applied to the dual-layer and triple-layer WLED packages. The attained results were examined with Mie-scattering theory and Lambert-Beer law. The dual-layer showed significant enhancement in color rendering index (CRI), in the range of approximate 80-90. Meanwhile, CRI in the triple-layer was lower and stayed around 66. In terms of color quality scale (CQS), a more overall color evaluating index, triple-layer structure helps the glass-based WLED achieve higher value than the dual-layer. The triple-layer is also beneficial to the luminous efficacy, according to the experimented results. Thus, the triple-layer structure can be used to strengthen the benefit of the glass matrix used in WLED products.

Corresponding Author:

Phan Xuan Le
Faculty of Engineering
Van Lang University
No. 45 Nguyen Khac Nhu Street, Ho Chi Minh City, Vietnam
Email: le.px@vlu.edu.vn

1. INTRODUCTION

In the illuminating field these days, white light-emitting diodes (WLEDs) have been considered as an excellent light source that can replace conventional fluorescent and incandescent lights in various illuminating fields, including general lightings, backlighting, and vehicle headlight. They have received such significant recognition due to their small size, high durability, high lighting efficiency, and being energy-saving and eco-green [1], [2]. According to researchers, not only does the luminous flux but the chromatic quality including color rendering index (CRI) also have great effects on human's psychology and physiology [3], [4]. Therefore, the color performance plays an indispensable role in achieving users' satisfaction. It is noted that a WLED with high CRI value has a continuous broad-band spectrum but the common WLED package, InGaN-based WLED using the mixture of yellow phosphor and resin, results in CRI just around 70. Researchers proposed integrating multiple phosphors into the silicone matrix to enhance CRI for WLED, and attained the resut above 85 [5], [6]. However, the thermal instability is one of the main problems that the high-power WLED using resin-based phosphors confronts. The heat emitted from the LED chip during the operation of a WLED device gradually damages the resin matrix, and from this the optical performance of the device is negatively affected. Thus, it is essential for manufacturers to have an alternative material whose matrix has high thermal stability to attain high performance. Several matrix materials were introduced with high thermal stability and average optical efficiency for WLED mixed phosphor base, including the ceramics matrix [7], [8] and glass matrix [9], [10]. These two matrixes are produced by applying recrystallizing method at high temperature (above 1000^{o}C), and this technique probably increases the cost of thermal-

durable phosphor fabrication. Thus, they are not favorable to WLED manufacturers. According to a previous study, directly integrating phosphor crystals into the glass matrix can lower the temperature of glass-based phosphor process to 680ºC, which is also beneficial to the manufacturing cost [11], [12]. In addition, this glass-based phosphor has high thermal-stable efficiency. Along with figuring out a way to attain cost-effective the glass-based phosphors, researches also aim at achieving high color rendering index (CRI) with this glass matrix. In a study, they pointed out that the reduction of phosphor interdiffusion can greatly enhance CRI value for glass-based phosphor WLEDs [13], [14]. Based on mentioned reports, we believe that using glass-based phosphor structure can boost the color rendering index and luminescence performance for pc-WLEDs. In this study, we aim to attain high color quality scale and luminous efficiency with multiple-layer remote phosphor structure utilizing sodium glass-based phosphors. As far as we concerned, color quality scale is more powerful than color rendering index in terms of evaluating color quality of a pc-WLED device. The sodium-based glass has high thermal stability and transparency, so is advantageous to these researched multiple glass-based phosphors WLEDs [15], [16]. Besides, the remote-phosphor structure is well-known for excellent luminous efficiency, so this structure is applied to form the novel glass-based WLED package. The phosphors dispersed into the sodium-based glass matrix are red ZnS:Te,Mn and green CdS:In phosphors, in addition to the yellow YAG:Ce phosphor. These phosphors were integrated with appropriate proportions. Several experiments were conducted on the dual-layer (DL) and triple-layer (TL) remote glass-based phosphor structures. The comparison between these two packages is drawn and shows considerable differences accompanying with significant enhancement in the adequacy of chromaticity and lumen output.

2. RESEARCH METHOD

2.1. Preparation of phosphor materials

We have to prepare the green CdS:In and red ZnS:Te,Mn phosphor materials to before blending them with the glass matrix. Their preparation processes must be carried out following an exact order. The composition of green CdS:In includes 99 mole% CdS and 1 mole% In_2O_3 with the weight of 1 g and 7.95 mg, respectively. The dry CdS and In powders are first placed in a quartz ampoule and then mixed vigorously with a Vortex mixer. After that, the quartz ampoule is sealed under vacuum, about 1 x 10 torr, and then annealed at 900ºC for 10 hours [17], [18]. After 10 hours, open the ampoule and take the mixture out for grinding into fine powder with a mortar and pestle. Next, the compound powder is placed in the quartz ampoule which is sealed and annealed under the same condition as the previous stage. As soon as the annealing time is finished, open the ampoule and one more time grind the compound into powder. It is noted that the attained compound must be in uniform light green color; if the compound has green light color but not uniform, it can be 10-hour annealed for the third time in a vacuum-sealed ampoule at 900ºC. The successfully attained green CdS:In phosphor has the greenish-yellow body color, and green emission that peaks at about 519 nm. Besides, green CdS:In phosphor is excited by all UV and by visible blue light. The preparation process of red ZnS:Te,Mn phosphor is less complicated than that of the green CdS:In particles. First, the composition of 94 mole% ZnS, 3 mole% ZnTe, 3 mole% MnO, and 10 mole% S is mixed and ground. The attained compound is going through a pre-sintering stage at 800ºC in N_2 for about 2 hours. After this stage, the compound is turned into powders and then ground again [19]. The next sintering process of this compound is carried out at 1200ºC in N_2 gas and lasts for 3 hours. The final ZnS:Te,Mn particles has red emission color with the peak emission at of 650 nm. In addition to that, in terms of excitation efficiency by UV, red ZnS:Te,Mn is excited by 280-380 nm UV and 450-540 nm blue green light.

2.2. Simulation process

The composition of sodium mother glass includes SiO_2 (60 mol%), Na_2CO_3 (25 mol%), Al_2O_3 (9 mol%), and CaO (6 mol%). These ingredients were blended uniformly, then the mixture was melted at 1300ºC, and finally cooled to the room temperature. Afterwards, the attained cullet glass was turned into powders by grinding and then screened to have a size of under 125μm. Red ZnS:Te,Mn and green CdS: In phosphor particles with a size of 10μm were mixed into glass powders to create glass phosphor precursor. After that, the precursor was sintered at the temperature of 680°C for 30 minutes, before going through an annealing process at 350ºC for about 3 hours. The phosphor-glass product was cooled to the room temperature [20], [21]. To form the multiple-layer glass-based remote phosphor structure, the cooled phosphor glass was cut into thin disks with a thickness of 0.08 mm, and a diameter of 15 mm. The red phosphor-glass disk was placed above the yellow phosphor layer in the dual-layer remote phosphor structure. In the triple-layer remote phosphor structure, the green glass-based phosphor film appeared in between the red glass-based phosphor and yellow phosphor classes, with the red phosphor at the top and the yellow phosphor at the bottom. The concentration of red phosphor in the glass matrix is changeable to observe the effects of yellow phosphor fluctuation on the WLED optical properties. The photoluminescence and

absorption spectrum of the glass-based phosphors, emitted by bare blue chips, were analyzed to attain the internal quantum yield. To measure the luminescence spectra of glass-phosphor WLED packages, we used a charge-coupled device detector configured on an integrating sphere calibrated with a Photo Research, Inc. PR-650 SpectraScan Colorimeter, see Figure 1. The chromatic evaluating parameters, including color rendering index (CRI), color coordinates, correlated color temperature (CCT), and lumen output values of pc-WLED packages using glass-based phosphors were investigated with the emission spectra and at the same driving current.

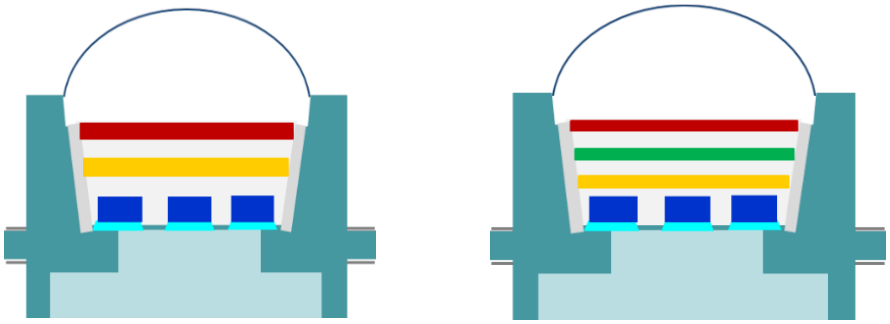

(a) (b)

Figure 1. Illustration of white LED multi-layer phosphorous structures, (a) Dual-layer phosphorus (DL), (b) triple-layer phosphorus (TL)

The concentration of yellow phosphor YAG:Ce^{3+} is varied following the change in concentrations of red phosphor in the glass-based phosphor layer to achieve the stability in average CCTs. Besides, concentrations of yellow phosphors are different at each distinguish CCT, which causes diverse internal scattering occurrences of WLED structures to happen and leads to the variations in lighting performance results. As presented in Figure 2, the phosphor concentration of YAG:Ce^{3+} in dual-layer WLED structure was higher than in triple-layer structure at any average CCT. Given that average CCTs of DL and TL structures are the same, the higher concentration of YAG:Ce^{3+} results in the increase of backscattering lights and then reduces the lumen efficiency. What is more, the color balance will be destroyed as the yellow phosphor concentration increases, which greatly damages the chromaticity of generated white lights. Therefore, the enhancement in color quality and luminous flux can be achieved provided that backscattering effects are reduced. This requirement can be attained by adding red-light components to the white-light generating process. In addition to the backscattering reduction, the improvement in lumen output can be fulfilled with the addition of green-light elements. As can be seen in Figure 3, the TL configuaration has the emission spectra significantly improved and better than that of DL configuration. Thus, it is possible to assume that the triple-layer glass-based phosphor structure can be used to attain the high color quality, lumen efficiency, and thermal stability for WLED products. We will discuss this assumption in detail in the next section.

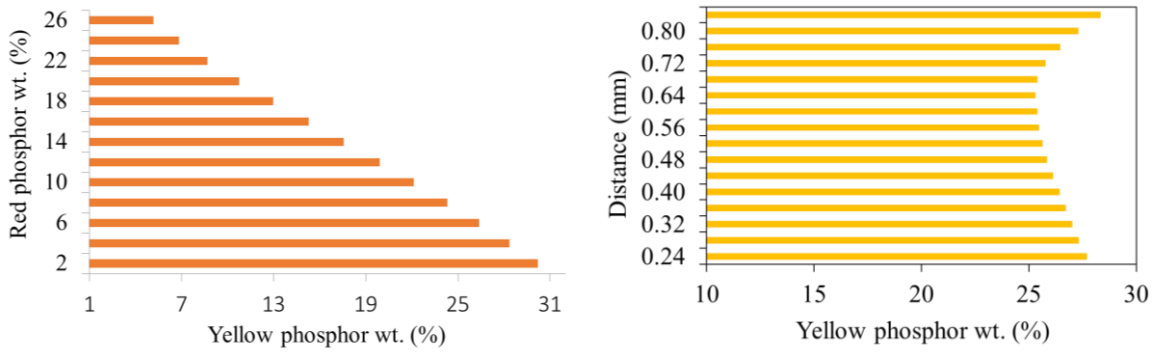

(a) (b)

Figure 2. The concentration of yellow YAG:Ce^{3+} phosphor in each remote phosphor structure, (a) DL, (b) TL

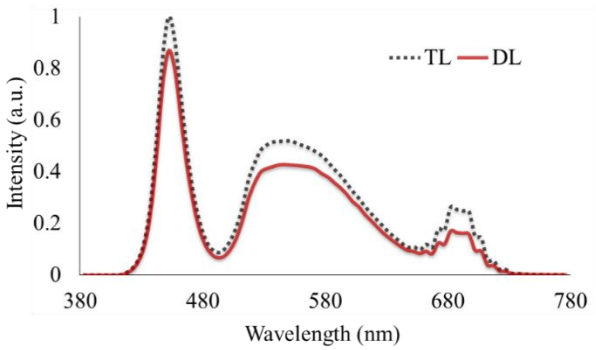

Figure 3. Emission spectra of phosphor configurations

3. RESULTS AND DISCUSSIONS

In Figure 4, CRI values of dual-layer and triple-layer simulation models were demonstrated. It is easy to see that the CRI of DL structure is superior to that of the TL one, and it increases with the rise of red phosphor concentration. Especially, the DL obtained the CRI peak, about 85, at 8500K CCT. This means the DL structure can gain high CRI for high-CCT WLED packages, which is one of difficult task for WLED using remote phosphor structure. Red ZnS:Te,Mn particles in glass-phosphor layer of the DL structure adds more red lights to the white-light generating process, leading to the increase in CRI. The TL structure showed stable CRI value, which remains at average level of about 66.

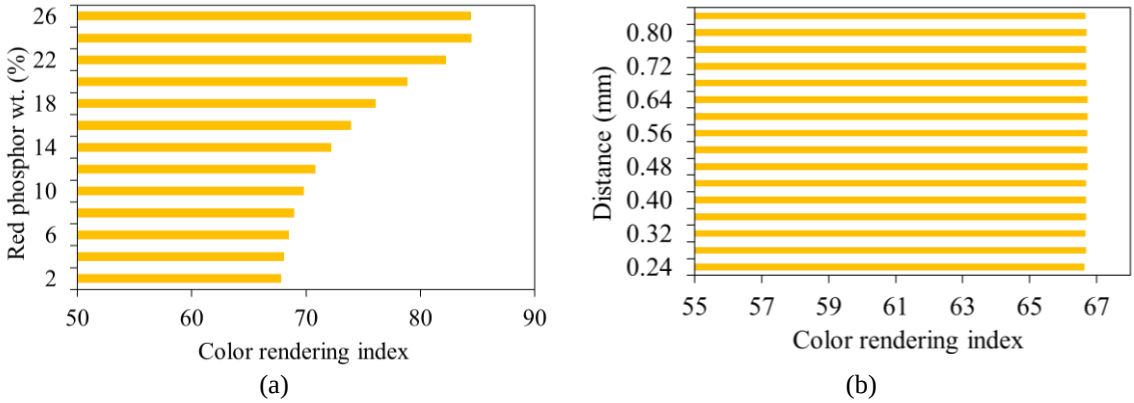

Figure 4. Color rendering indexes of phosphor configurations corresponding to ACCTs, (a) DL, (b) TL

Recently, aside high color rendering index, researchers have aimed at excellent color quality scale (CQS). They stated that color quality scale is superior than CRI because CRI is one of three elements comprising CQS. The other two factors are viewers' preference and chromaticity coordinate. Thus, a WLED having high CQS value means it has high color quality. Figure 5 showed the CQS value obtained in two-layered and three-layered structures. The TL structure presented better CQS than the DL model as the chromatic balance among three basic color components of white-lights: red, green, and yellow was formed. At this point, three-layered packaging design is more suitable to be applied in WLED packages for higher color adequacy.

The TL structure can effectively boost the color quality, but there is no assurance that the luminous flux will be elevated simultaneously because it is noted that if the chromatic homogeneity increases, the lumen output will decrease. Therefore, to confirm the benefits of the TL to the luminous flux, we carried out a mathematic system of transmitted blue light and converted yellow light in the triple-layer structure and presented below as the following. The transmitted blue light and converted yellow light in dual-layer structure with each phosphor layer having the thickness of *h*, the calculation is expressed as [22], [23]:

$$PB_2 = PB_0 e^{-\alpha_{B_2} h} e^{-\alpha_{B_2} h} = PB_0 e^{-2\alpha_{B_2} h} \quad (1)$$

$$PY_2 = \frac{1}{2}\frac{\beta_2 PB_0}{\alpha_{B_2}-\alpha_{Y_2}}[e^{-\alpha_{Y_2}h} - e^{-\alpha_{B_2}h}]\,e^{-\alpha_{Y_2}h} + \frac{1}{2}\frac{\beta_2 PB_0}{\alpha_{B_2}-\alpha_{Y_2}}[e^{-\alpha_{Y_2}h} - e^{-\alpha_{B_2}h}]$$
$$= \frac{1}{2}\frac{\beta_2 PB_0}{\alpha_{B_2}-\alpha_{Y_2}}[e^{-2\alpha_{Y_1}h} - e^{-2\alpha_{B_1}h}] \quad (2)$$

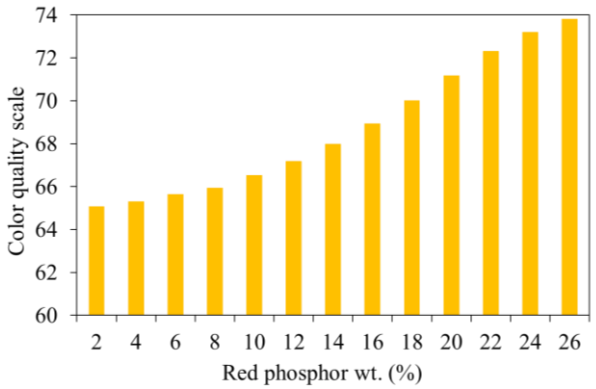

Figure 5. Color quality scale of the corresponding ACCTs phosphor configurations

The TL with phosphor layer thickness of $\frac{2}{3}h$, these mentioned blue light and yellow light can be computed by:

$$PB_3 = PB_0.e^{-\alpha_{B_2}\frac{2h}{3}}.e^{-\alpha_{B_2}\frac{2h}{3}}.e^{-\alpha_{B_2}\frac{2h}{3}} = PB_0.e^{-2\alpha_{B_3}h} \quad (3)$$

$$PY'_3 = \frac{1}{2}\frac{\beta_3 PB_0}{\alpha_{B_3}-\alpha_{Y_3}}[e^{-\alpha_{Y_3}\frac{2h}{3}} - e^{-\alpha_{B_3}\frac{2h}{3}}]\,e^{-\alpha_{Y_3}\frac{2h}{3}} + \frac{1}{2}\frac{\beta_3 PB_0 e^{-\alpha_{B_3}\frac{2h}{3}}}{\alpha_{B_3}-\alpha_{Y_3}}[e^{-\alpha_{Y_3}\frac{2h}{3}} - e^{-\alpha_{B_3}\frac{2h}{3}}]$$
$$= \frac{1}{2}\frac{\beta_3 PB_0}{\alpha_{B_3}-\alpha_{Y_3}}[e^{-\alpha_{Y_3}\frac{4h}{3}} - e^{-2\alpha_{B_3}\frac{4h}{3}}] \quad (4)$$

$$PY_3 = PY'_3.e^{-\alpha_{Y_3}\frac{2h}{3}} + PB_0.e^{-2\alpha_{B_3}\frac{4h}{3}}\frac{1}{2}\frac{\beta_3}{\alpha_{B_3}-\alpha_{Y_3}}[e^{-\alpha_{Y_3}\frac{2h}{3}} - e^{-\alpha_{B_3}\frac{2h}{3}}]$$
$$= \frac{1}{2}\frac{\beta_3 PB_0}{\alpha_{B_3}-\alpha_{Y_3}}[e^{-\alpha_{Y_3}\frac{4h}{3}} - e^{-\alpha_{B_3}\frac{4h}{3}}]\,e^{-\alpha_{Y_3}\frac{2h}{3}} + \frac{1}{2}\frac{\beta_3 PB_0 e^{-\alpha_{B_3}\frac{4h}{3}}}{\alpha_{B_3}-\alpha_{Y_3}}[e^{-\alpha_{Y_3}\frac{2h}{3}} - e^{-\alpha_{B_3}\frac{2h}{3}}] \quad (5)$$
$$= \frac{1}{2}\frac{\beta_3 PB_0}{\alpha_{B_3}-\alpha_{Y_3}}[e^{-\alpha_{Y_3}h} - e^{-2\alpha_{B_3}h}]$$

Where *h* presents the phosphor layer's thickness, "2" and "3" are the subscripts describing the dual-layer and triple-layer phosphor configurations, respectively. β is the conversion coefficient for the blue light that converts to the yellow light, and γ is the reflection coefficient of the yellow light. *PB* demonstrates the intensity of blue lights, and *PY* shows the intensity of yellow lights. PB_0 describes the light intensity from the blue LED chip which includes both blue and yellow light intensities. α_B and α_Y present the fractions of the energy loss of blue and yellow lights during their propagation in the phosphor layer respectively. Besides, PY'_3 in (4) is the yellow transmitted light through two phosphor layers.
The lighting performance achieved with TL structure is greatly heightened, even higher than with DL model:

$$\frac{(PB_3-PY_3)-(PB_2+PY_2)}{(PB_2+PY_2)} > \frac{e^{-2\alpha_{B_3}h} - e^{-2\alpha_{B_2}h}}{e^{-2\alpha_{Y_3}h} - e^{-2\alpha_{B_2}h}} > 0 \quad (6)$$

Mie-scattering theory is used to study the scattering events inside remote-phosphor WLEDs and support the computation of scattering cross section C_{sca} for spherical particles. Additionally, Lambert-Beer law is utilized to compute the transmitted light power [24], [25]:

$$I = I_0\, exp(-\mu_{ext}L) \quad (7)$$

In (7), I_0 presents the incident light power; L is used to indicate the thickness of a phosphor layer (mm), while μ_{ext} describes the extinction coefficient. In addition, the expression for calculating μ_{ext} can be demonstrated as follows: $\mu_{ext}=N_r.C_{ext}$, in which N_r (mm^{-3}) and C_{ext} (mm^2) indicate the number density distribution and the extinction cross-section of phosphor particles, respectively.

Based on (6), it can be said that triple-layer glass-based remote phosphor structure probably results in better luminous efficiency than the dual-layer structure. This result was also presented in Figure 6. So, we can assure that the triple-layer module can perfectly improve the color and luminous performances at the same time. This impressive advancement of TL structure can be attributed to the higher emission spectrum in 500 nm-600 nm wavelength band, which can be seen in Figure 3. The greater emission intensity is the result of the significant reduction of yellow phosphor concentration to maintain the CCT for triple-layer WLEDs. When the yellow phosphor contents were largely reduced, the TL can diminish the backscattering events, help the transmission through the other phosphor layers of the light emitted from blue chips become more easier, which means that the blue-chip emitting light can be converted more effectively. Thus, TL structure can achieve better luminous efficacy than DL configuration. The color uniformity is one of the most important factors to the color quality of WLED devices. The common way to enhance the color uniformity is to improve the scattering of lights inside the LED package. Thus, scattering enhancing particles (SEPs), including SiO_2, $CaCO_3$, etc., were applied to fabricate remote phosphor configuration. Though the color uniformity was improved, the luminous flux showed considerable degradation. However, the triple-layer structure can minimize the disadvantage in lumen output of the WLED. The benefits of using red ZnS:Te,Mn and green CdS:In phosphor in TL design are boosted scattering ability and increased proportions of green and red light components inside the WLED, resulting in better quality of white light. Besides, the remote phosphor structure is beneficial to the luminous flux as it effectively reduces the backscattering effect which is the primary factor causing the luminous efficiency to decline. However, according to (7), to manage to accomplish the best power transmission, the phosphor must be added with a suitable concentration, which will be investigated in our other future works.

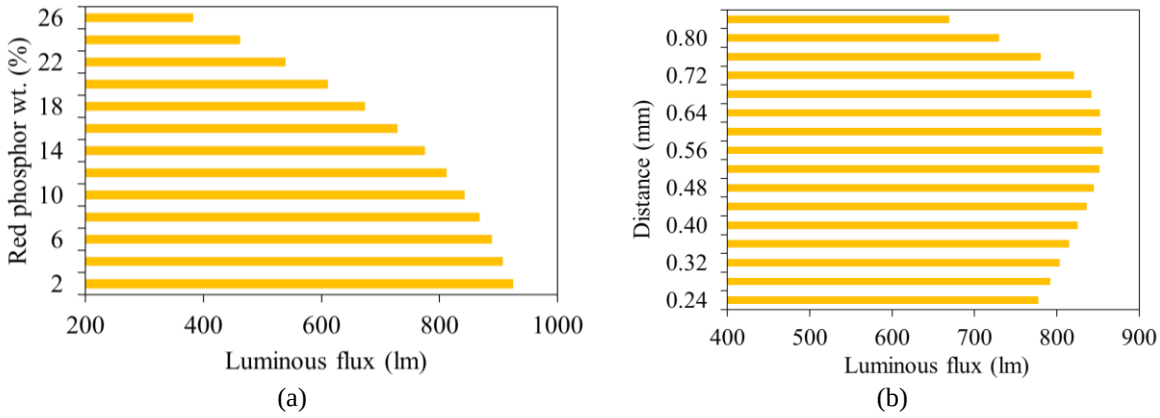

Figure 6. Luminous output (LO) of phosphor configurations corresponding to ACCTs, (a) DL, (b) TL

In Figure 7, the deviations in correlated color temperature (D-CCT) of DL and TL structures were illustrated. The D-CCT value in TL configuration is lower than in DL model. This D-CCT difference is more obvious when they were applied to WLED with high average CCT, for example 8500 K CCT. The lower the D-CCT value the better the color homogeneity, due to the scattering enhancement when there are more phosphor layers applied. As mentioned before, the increase of scattering events leads to the reduction of luminous flux. However, the advantages of reducing backscattering effects are more than this reduction in luminous flux. Moreover, the lumen efficiency of the TL is better than the DL structure. Therefore, the triple-layer structure can be used to fabricate WLED with high color quality and improved lumen efficacy.

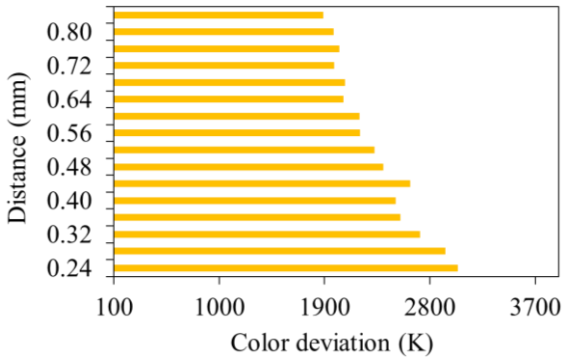

Figure 7. Correlated color temperature deviation (D-CCT) of remote phosphor configurations corresponding to ACCTs

4. CONCLUSION

In this paper, we developed WLED models using multi-layer remote phosphor with the phosphor layer formed by integrating red and green phosphor particles into the glass matrix. The glass-based phosphor can help the WLED attain high thermal stability while the remote structure can enhance the lumen efficiency. The two experimented remote phosphor modules are the dual-layer structure using a red phosphor/glass layer, and the triple-layer using both green and red phosphor-glass layers, in addition to the original yellow phosphor YAG:Ce^{3+} layer. The results showed that the dual-layer is superior in color rendering index but inferior in color quality scale, in comparison with the triple-layer structure. Besides better CQS, the triple-layer structure has greater reduction in color deviation due to the enhanced scattering ability. Not only is the color quality promoted but also the lumen efficiency is better when using the triple-layer structure, which can be attributed greatly to the considerable backscattering minimization. In short, the triple-layer remote phosphor with glass-based phosphor layers can be utilized in WLED production for a high-power pc-WLED generation with high thermal durability, better color adequacy, great lumen efficacy, and can be applied widely in not only outdoor but also indoor lightings.

REFERENCES

[1] Tang Wei, Wang Bo, Chen Yan, Chen Yeqing, Lin Jun, and Zeng Qingguang, "Single Pr^{3+}-activated high-color-stability fluoride white-light phosphor for white-light-emitting diodes," *Optical Materials Express*, vol. 9, pp. 223-233, 2019, doi: 10.1364/OME.9.000223.

[2] P. P. Li, *et al.*, "Very high external quantum efficiency and wall-plug efficiency 527 nm InGaN green LEDs by MOCVD," *Optics Express*, vol. 26, pp. 33108-33115, 2018, doi: 10.1364/OE.26.033108.

[3] T. Han, *et al.*, "Spectral broadening of a single Ce3+-doped garnet by chemical unit cosubstitution for near ultraviolet LED," *Optical Materials Express*, vol. 8, pp. 3761-3769, 2018, doi: 10.1364/OME.8.003761.

[4] X. Liu, *et al.*, "Laser-based white-light source for high-speed underwater wireless optical communication and high-efficiency underwater solid-state lighting," *Optics Express*, vol. 26, pp. 19259-19274, 2018, doi: 10.1364/OE.26.019259.

[5] T. Zhang, X. Zhang, B. Ding, J. Shen, Y. Hu, H. Gu, "Homo-epitaxial secondary growth of ZnO nanowire arrays for a UV-free warm white light-emitting diode application," *Applied Optics*, vol. 59, no. 8, pp. 2498-2504, 2020, doi: 10.1364/AO.385656.

[6] M. A. Juratli, *et al.*, "Noninvasive label-free detection of circulating white and red blood clots in deep vessels with a focused photoacoustic probe," *Biomedical Optics Express*, vol. 9, no. 11, pp. 5667-5677, 2018, doi: 10.1364/BOE.9.005667.

[7] S. K. Abeysekera, V. Kalavally, M. Ooi, Y. C. Kuang, "Impact of circadian tuning on the illuminance and color uniformity of a multichannel luminaire with spatially optimized LED placement," *Optics Express*, vol. 28, no. 1, pp. 130-145, 2020.

[8] O. H. Kwon, J. S. Kim, J. W. Jang, Y. S. Cho, "Simple prismatic patterning approach for nearly room-temperature processed planar remote phosphor layers for enhanced white luminescence efficiency," *Optical Materials Express*, vol. 8, no. 10, pp. 3230-3237, 2018, doi: 10.1364/OME.8.003230.

[9] S. Cincotta, C. He, A. Neild, J. Armstrong, "High angular resolution visible light positioning using a quadrant photodiode angular diversity aperture receiver (QADA)," *Optics express*, vol. 26, no. 7, pp. 9230-9242, 2018, doi: 10.1364/OE.26.009230.

[10] L. V. Labunets, A. B. Borzov, and I. M. Akhmetov, "Regularized parametric model of the angular distribution of the brightness factor of a rough surface," *Journal of Optical Technology*, vol. 86, no. 10, pp. 618-626, 2019, doi: 10.1364/JOT.86.000618.

[11] T. DeLawyer, M. Tayon, C. Yu, S. L. Buck, "Contrast-dependent red-green balance shifts depend on S-cone activity," *Journal of the Optical Society of America A,* vol. 35, no. 4, pp. B114-B121, 2018, doi: 10.1364/JOSAA.35.00B114.
[12] Z. Li, J. Zheng, J. Li, W. Zhan, Y. Tang, "Efficiency enhancement of quantum dot–phosphor hybrid white-light-emitting diodes using a centrifugation-based quasi-horizontal separation structure," *Optics Express,* vol. 28, no. 9, pp. 13279-13289, 2020, doi: 10.1364/OE.392900.
[13] T. Shao, *et al.*, "Understanding the role of fluorine-containing plasma on optical properties of fused silica optics during the combined process of RIE and DCE," *Optics Express,* vol. 27, no. 16, pp. 23307-23320, 2019, doi: 10.1364/OE.27.023307.
[14] Y. Tian, *et al.*, "Study of composite Al_2O_3-Ce:$Y_3Mg_{1.8}Al_{1.4}Si_{1.8}O_{12}$ ceramic phosphors," *Optics letters*, vol. 44, no. 19, pp. 4845-4848, 2019, doi: 10.1364/OL.44.004845.
[15] Alina Keller, Piotr Bialecki, Torsten Johannes Wilhelm, and Marcus Klaus Vetter, "Diffuse reflectance spectroscopy of human liver tumor specimens-towards a tissue differentiating optical biopsy needle using light emitting diodes," *Biomedical Optics Express,* vol. 9, no. 3, pp. 1069-1081, 2018, doi: 10.1364/BOE.9.001069.
[16] C. H. Lin, *et al.*, "Hybrid-type white LEDs based on inorganic halide perovskite QDs: candidates for wide color gamut display backlights," *Photonics Research,* vol. 7, no. 5, pp. 579-585, 2019, doi: 10.1364/PRJ.7.000579.
[17] Y. P. Chang, *et al.*, "An advanced laser headlight module employing highly reliable glass phosphor," *Optics Express*, vol. 27, pp. 1808-1815, 2019, doi: 10.1364/OE.27.001808.
[18] Y. C. Jen, *et al.*, "Design of an energy-efficient marine signal light based on white LEDs," *OSA Continuum,* vol. 2, pp. 2460-2469, 2019, doi: 10.1364/OSAC.2.002460.
[19] X. Ding, *et al.*, "Improving the optical performance of multi-chip LEDs by using patterned phosphor configurations," *Optics Express*, vol. 26, no. 6, pp. A283-A292, 2018, doi: 10.1364/OE.26.00A283.
[20] Yan Sun, Chi Zhang, Yanling Yang, Hongmei Ma, and Yubao Sun, "Improving the Color Gamut of a Liquid-crystal Display by Using a Bandpass Filter," *Current Optics and Photonics*, vol. 3, no. 6, pp. 590-596, 2019, doi: 10.1364/COPP.3.000590.
[21] J. Hao, H. L. Ke, L. Jing, Q. Sun, R. T. Sun, "Prediction of lifetime by lumen degradation and color shift for LED lamps, in a non-accelerated reliability test over 20,000 h," *Applied Optics,* vol. 58, no. 7, pp. 1855-1861, 2019, doi: 10.1364/AO.58.001855.
[22] Rada Deeb, Joost Van de Weijer, Damien Muselet, Mathieu Hebert, and Alain Tremeau, "Deep spectral reflectance and illuminant estimation from self-interreflections," *Journal of the Optical Society of America A,* vol. 36, no. 1, pp. 105-114, 2019, doi: 10.1364/JOSAA.36.000105.
[23] M. Hu, *et al.*, "Broadband emission of double perovskite Cs2Na0.4Ag0.6In0.995Bi0.005Cl6:Mn2+ for single-phosphor white-light-emitting diodes," *Optics Letters,* vol. 44, no. 19, pp. 4757-4760, 2019, doi: 10.1364/OL.44.004757.
[24] B. G. Assefa, *et al.*, "Realizing freeform lenses using an optics 3D-printer for industrial based tailored irradiance distribution," *OSA Continuum,* vol. 2, pp. 690-702, 2019, doi: 10.1364/OSAC.2.000690.
[25] Z. Huang, Q. Liu, M. R. Pointer, W. Chen, Y. Liu, Y. Wang, "Color quality evaluation of Chinese bronzeware in typical museum lighting," *Journal of the Optical Society of America A,* vol. 37, pp. A170-A180, 2020, doi: 10.1364/JOSAA.381498.